

DFT study of structure stability and elasticity of wadsleyite II

This article has been downloaded from IOPscience. Please scroll down to see the full text article.

2010 J. Phys.: Condens. Matter 22 145402

(<http://iopscience.iop.org/0953-8984/22/14/145402>)

View [the table of contents for this issue](#), or go to the [journal homepage](#) for more

Download details:

IP Address: 129.252.86.83

The article was downloaded on 30/05/2010 at 07:43

Please note that [terms and conditions apply](#).

DFT study of structure stability and elasticity of wadsleyite II

K Tokár, P T Jochym, K Parlinski, J Łażewski, P Piekarczyk and M Sternik

Institute of Nuclear Physics, Polish Academy of Sciences, Radzikowskiego 152, 31-342 Cracow, Poland

E-mail: tokar@wolf.ifj.edu.pl

Received 7 December 2009, in final form 8 February 2010

Published 19 March 2010

Online at stacks.iop.org/JPhysCM/22/145402

Abstract

The structure and stability properties of wadsleyite II as the new phase of Mg_2SiO_4 has been studied at high pressure by the DFT method. The pressure range corresponds to the transition zone in the Earth. At zero pressure the calculated lattice parameters of the wadsleyite II structure are $a = 5.749 \text{ \AA}$, $b = 28.791 \text{ \AA}$ and $c = 8.289 \text{ \AA}$ with the density $\rho = 3406 \text{ kg m}^{-3}$. The third order Birch–Murnaghan equation of state has been determined for the structure with isothermal bulk moduli $K_T = 160.1 \text{ GPa}$ and $K'_T = 4.3$ at a pressure range up to 50 GPa. The elasticity tensor coefficients $C_{ij}(P)$, as well as the compressional and shear wave velocities and their pressure derivatives, have been calculated using the deformation method at a range of pressures up to 25 GPa. The results agree with the experimental data and structure properties of the wadsleyite II model. The properties of the wadsleyite II phase are very close to the wadsleyite phase.

(Some figures in this article are in colour only in the electronic version)

1. Introduction

The major components of the upper mantle and the transition zone (at 410–660 km) are considered to be magnesium and magnesium–iron silicate forms of $(\text{Mg}_{2-x}\text{Fe}_x\text{SiO}_4)$: forsterite, wadsleyite and ringwoodite [1, 2]. The transition interval between upper (wadsleyite) and lower (ringwoodite) layers is at the depth of 520 km with corresponding pressure 17–19 GPa [2, 3]. A new, high pressure, hydrous magnesium silicate phase wadsleyite II was experimentally observed at these conditions. The synthesis of a sample of wadsleyite II structure has been first reported by Smyth *et al* [4]. It is a hydrous magnesium iron silicate spineloid which contains about 2.0–2.7 wt% of H_2O . This phase occurs abundantly in hydrous experiments on multi-component mantle compositions under the conditions expected in the transition zone. The presence of hydrogen in rock compounds has a major effect on important properties such as melting, strength, elastic constants and seismic velocities [4]. The structure of wadsleyite II is similar to the spineloid IV phase found in the nickel aluminosilicates by Horioka *et al* [5] and Akaogi *et al* [6]. The detected structure is based on a cubic, close packed array of oxygens, similar to the one present in wadsleyite ($\beta\text{-Mg}_2\text{SiO}_4$) and ringwoodite ($\gamma\text{-Mg}_2\text{SiO}_4$) [4].

Wadsleyite contains only Si_2O_7 groups and no isolated Si-tetrahedra in its structure. Wadsleyite II, on the other hand, has one fifth of Si atoms in isolated tetrahedra and four fifths in Si_2O_7 groups, as is typical for spinelloids IV [5]. The sites of these groups in the crystal represent highly distorted tetrahedra with a very long distance between Si and the bridging oxygen atom [7]. It is clearly a new structure, although one very closely related to that of wadsleyite [4]. The space group symmetry of the crystal structure has been identified as *Imma* with the orthorhombic body-centered lattice and the unit cell parameters: $a = 5.6884 \text{ \AA}$, $b = 28.9238 \text{ \AA}$ and $c = 8.2382 \text{ \AA}$ for the sample under the conditions of synthesis $T = 1400 \text{ }^\circ\text{C}$, and $P = 18.5 \text{ GPa}$. The lattice constants a and c are approximately those of wadsleyite, whereas b is 2.5 times larger than in wadsleyite [4].

The presence of the wadsleyite II phase could obscure the seismic expression of the phase boundary between the wadsleyite and ringwoodite near 525 km, where it can occur as an intermediate phase [7]. Under the conditions of a pyrolite mantle with 1400 °C temperature, the wadsleyite to ringwoodite phase transition is characterized by seismic observation data [8], as a reflector near 520 km depth, about 20 km thick and with a density jump of 2.1% and impedance jumps of 2.4% and 3.1% for the P and S waves respectively.

In this study we have concentrated on the first principles investigation of the lattice stability properties and elasticity of a pure, anhydrous, Mg_2SiO_4 structure of wadsleyite II, which was reported from experiments as a new phase in this orthosilicate system [4]. These properties could play an important role in the interpretation of seismic data and development of geodynamical models of the transition zone in the Earth [9].

2. Calculation details

We have used density functional theory (DFT), applying the generalized gradient approximation (GGA) with the Perdew–Burke–Ernzerhof (PBE) functional [10] and Projector Augmented Wave approach with GGA-PBE potentials as implemented in the VASP package [11].

The considered model of the crystal structure of wadsleyite II is similar to that of spinelloid IV, and has an orthorhombic cell with $Imma$ (#74) symmetry, with chemical formula Mg_2SiO_4 and number of formulae $Z = 20$ in the unit cell. The geometry of the model structure has been optimized in the range of pressures between 0 and 50 GPa. These optimizations were performed in the $1 \times 1 \times 1$ supercell containing 140 atoms. The \mathbf{k} -point space was sampled by a $2 \times 2 \times 2$ Monkhorst–Pack mesh [12] with eight irreducible \mathbf{k} -points. The energy cutoff for expansion of the wavefunctions to plane waves was chosen at 500 eV. The electronic and ionic optimizations were continued until the energy differences between successive electronic and ionic relaxations were less than 10^{-7} and 10^{-6} eV respectively.

The stability of the crystal structure has been checked from the lattice dynamical properties at several pressures in the interval between $P = 0$ and 30 GPa. The lattice dynamics has been computed using a direct method [13], as implemented in the PHONON software [14]. The Hellmann–Feynman (HF) forces used in construction of the dynamical matrix (DM) have been derived from the lattice with selected atoms displaced from the equilibrium positions. The third order Birch–Murnaghan equation of state (BM EOS) has been parametrized using the least squares regression method applied to the volume versus pressure data $V_{\text{cell}}(P)$. To increase the accuracy of the fitting procedure we have extended the range of pressures for structural calculations to 50 GPa.

The elasticity properties of wadsleyite II are described by nine independent components $C_{ij}(P)$ of the elasticity tensor appropriate to a body-centered orthorhombic cell with space symmetry group $Imma$. The generalized Hook law for crystals has been used for determination of the elasticity tensor [15]. The unit cell was deformed by basic axial and shear deformations, and then the stress tensor was calculated. The elasticity tensor components $C_{ij}(P)$ have been determined for the interval of pressures up to $P = 25$ GPa, from a system of linear equations, which relate the strain and stress tensors.

The compressional v_p and shear v_s wave velocity in the anhydrous wadsleyite II structure have been calculated from additional elasticity characteristics such as the bulk modulus K , Young's modulus E , strain modulus μ and Poisson's ratio σ . These additional moduli are in turn defined

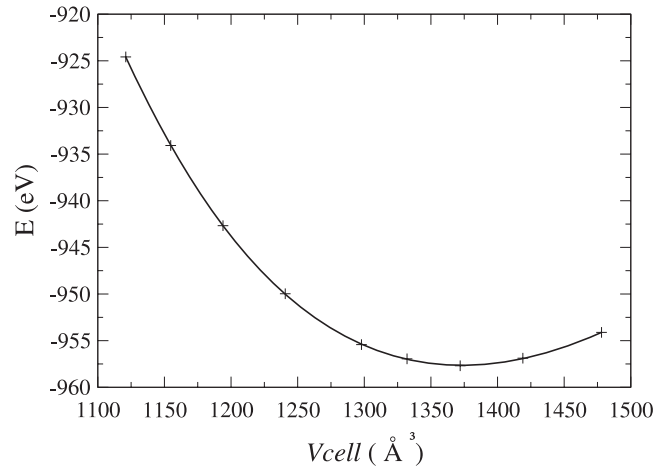


Figure 1. The energy of the wadsleyite II structure as a function of the unit cell volume for a range of pressures up to 50 GPa. For zero external pressure the structure has its minimum of ground state energy at the unit cell volume 1372 \AA^3 . The crosses denote the calculated points and the solid line is the fourth order polynomial fit to the data.

by the elasticity tensor components $C_{ij}(P)$. The calculated values of lattice and elasticity parameters of the wadsleyite II model structure have been compared with the experimental data of hydrous phase wadsleyite II and anhydrous and hydrous phases of wadsleyite.

3. Lattice parameters

The dependence of the static energy on the unit cell volume is presented in figure 1. We have used a fourth order polynomial fit to describe the shape of the function and find the minimum. The structure has minimum ground state energy for the unit cell volume 1372 \AA^3 , the corresponding lattice constants being: $a = 5.749 \text{ \AA}$, $b = 28.791 \text{ \AA}$ and $c = 8.289 \text{ \AA}$. The experimental cell volume of the hydrous wadsleyite II sample is 1359 \AA^3 , which amounts to an about 1% relative difference between the calculated and experimental volume [7]. The calculated lattice constants dependence on the pressure is depicted in figure 2. From comparison with the experimental lattice constants of the hydrous wadsleyite II it follows that the computed values of a and c are close to the experimental data measured in the pressure interval up to 10.6 GPa [7]. The b axis shows slightly different compressional behavior—in calculation it is almost identical to the a axis while in experiment it has a compressibility between axes a and c .

The crystal density has been determined for all calculated cell volumes, and its values are included in table 1. The value of calculated density corresponding to the zero pressure is $\rho_0 = 3406 \text{ kg m}^{-3}$, which is close to the densities of the synthesized hydrous samples of magnesium–iron wadsleyite II: 3511 and 3495 kg m^{-3} obtained by Smyth *et al* [4]. On the other hand, these experimental densities of the wadsleyite II phase extrapolated to the iron free compositions gave 3383 kg m^{-3} and 3337 kg m^{-3} respectively, which represents about 2% relative difference between the calculation and experimental results of the Smyth group [4].

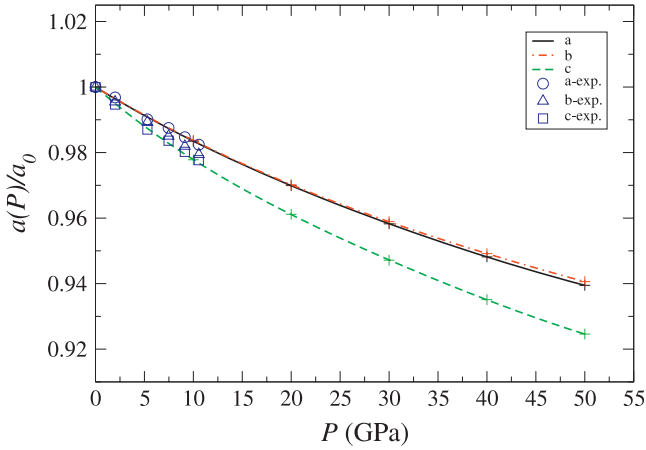


Figure 2. Lattice constants of anhydrous wadsleyite II as a function of pressure. The dashed–dotted, dashed and solid lines depict the calculated relative values for a , b and c , respectively. The circles, triangles up and squares represent the experimental relative lattice parameters for the hydrous phase of wadsleyite II (data from [7]).

The non-equivalent atom positions described by fractional coordinates in the wadsleyite II crystal unit cell have been compared with the measured structure of Smyth [7] in table 2. The optimized lattice structure at zero pressure is close to the experimentally determined structure and the relative differences between the coordinates are below 1%.

4. Structure stability

The DM for the lattice was constructed from inter-atomic forces, taking crystal symmetry into account. The set of HF forces acting on atoms in the supercell has been determined from single-point calculations for the structure with non-equivalent atoms displaced one by one from their equilibrium positions by 0.03 Å. The collected data has been used to determine vibrational modes by application of the direct

Table 1. Calculated lattice parameters, unit cell volumes and density of the wadsleyite II structure of Mg_2SiO_4 at pressures between 0 and 50 GPa.

P (GPa)	a (Å)	b (Å)	c (Å)	V (Å ³)	ρ (kg m ⁻³)
0	5.749	28.791	8.289	1372	3406
10	5.654	28.322	8.105	1298	3600
20	5.576	27.932	7.967	1241	3766
30	5.509	27.608	7.851	1194	3913
40	5.451	27.327	7.751	1155	4047
50	5.401	27.081	7.604	1121	4168

method [13, 14]. For the optimized structures the phonon frequencies have been calculated and the phonon density of states (PDOS) $g(\omega)$ has been determined by sampling of the Brillouin zone [16] at 5000 randomly generated points. The PDOS spectra of the wadsleyite II structure computed for pressures $P = 0\text{--}30$ GPa are presented in figure 3. It is clear from the PDOS that there are no imaginary phonon modes in the calculated spectra of wadsleyite II. This indicates that the spinelloid IV like structure of wadsleyite II (Mg_2SiO_4) is stable for pressures between 0 and 30 GPa.

5. Equation of state

The computed relative cell volume (V/V_0 , where V_0 is zero pressure volume) dependence on pressure is plotted in figure 4 and compared with experimental data of a hydrous wadsleyite II sample measured by Smyth *et al* [7]. The zero pressure unit cell volume of wadsleyite II has been estimated as $V_0 = 1372 \text{ \AA}^3$. The plot in figure 4 includes a fit of a third order BM EOS to the calculated data:

$$P = \frac{3}{2}K_T \left[\left(\frac{V_0}{V} \right)^{\frac{2}{3}} - \left(\frac{V_0}{V} \right)^{\frac{5}{3}} \right] \times \left[1 - \frac{3}{4}(4 - K'_T) \left(\left(\frac{V_0}{V} \right)^{\frac{2}{3}} - 1 \right) \right], \quad (1)$$

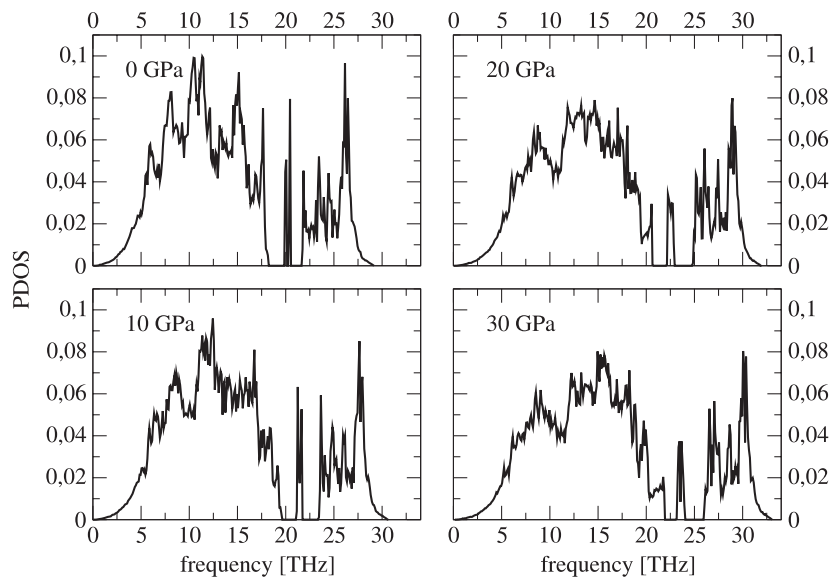


Figure 3. The lattice dynamics of wadsleyite II: phonon density of states (PDOS) calculated at pressures up to 30 GPa.

Table 2. Calculated fractional atom positions in the unit cell of wadsleyite II (at $P = 0$ GPa) are compared with the experimental data (sample 1 in [7]). The a , b , c are the appropriate lattice constants. Deltas represent absolute differences between the experimental and calculated position coordinates: ($\Delta_x = a_{\text{exp}} \cdot |x_{\text{exp}}/a_{\text{exp}} - x_{\text{cal}}/a_{\text{cal}}|$).

Atom	Experimental			Calculated			Differences		
	x/a	y/b	z/c	x/a	y/b	z/c	Δ_x (Å)	Δ_y (Å)	Δ_z (Å)
Mg1	0.2500	0.2500	0.7500	0.2500	0.2500	0.7500	0.000	0.000	0.000
Mg2	0.5000	0.1999	0.4938	0.5000	0.2003	0.4930	0.000	0.012	0.007
Mg3	0.5000	0.1002	0.5287	0.5000	0.1002	0.5303	0.000	0.002	0.013
Mg4	0.5000	0.0000	0.5000	0.5000	0.0000	0.5000	0.000	0.000	0.000
Mg5	0.2500	0.1499	0.2500	0.2500	0.1487	0.2500	0.000	0.035	0.000
Mg6	0.2500	0.0488	0.2500	0.2500	0.0510	0.2500	0.000	0.063	0.000
Si1	0.0000	0.2500	0.3774	0.0000	0.2500	0.3757	0.000	0.000	0.014
Si2	0.0000	0.1525	0.6167	0.0000	0.1528	0.6167	0.000	0.010	0.000
Si3	0.0000	0.0487	0.6157	0.0000	0.0481	0.6165	0.000	0.018	0.007
O1	0.0000	0.9951	0.2570	0.0000	0.9960	0.2552	0.000	0.026	0.015
O2	0.0000	0.0996	0.2246	0.0000	0.0998	0.2161	0.000	0.007	0.070
O3	0.0000	0.2030	0.2598	0.0000	0.2027	0.2588	0.000	0.008	0.008
O4	0.2377	0.0501	0.5056	0.2393	0.0492	0.5073	0.009	0.026	0.014
O5	0.2411	0.1507	0.5050	0.2400	0.1513	0.5086	0.006	0.020	0.029
O6	0.2416	0.2500	0.4956	0.2373	0.2500	0.4959	0.024	0.000	0.003
O7	0.0000	0.0999	0.7174	0.0000	0.1004	0.7168	0.000	0.016	0.005
O8	0.0000	0.1965	0.7468	0.0000	0.1971	0.7464	0.000	0.017	0.003

where V_0 is the unit cell volume at zero pressure, and V is the volume at P , K_T is isothermal bulk modulus and K'_T its pressure derivative [1]. The parameters obtained from the fitted BM EOS function are the isothermal bulk modulus: $K_T = 160.1$ GPa and its derivative $K'_T = 4.3$. This result is an approximation valid for the static lattice structure calculated at temperature $T = 0$ K and without a phonon zero-point contribution. These values are close to the experimental results for hydrous wadsleyite II moduli extrapolated to the anhydrous composition: $K_T = 167 \pm 10$ GPa [7]. Furthermore, the computed bulk moduli are also close to experimental values obtained for anhydrous wadsleyite [17]. The comprehensive comparison of the isothermal bulk moduli K_T for the hydrous and anhydrous phases of wadsleyite and wadsleyite II is included in table 3. From previous studies it follows that the bulk modulus is sensitive to the content of water, and the bulk modulus is diminished by increased concentration of H_2O in the wadsleyite and wadsleyite II phases [7, 18, 19].

6. Elasticity coefficients

The orthorhombic structure of wadsleyite II has nine independent components of the elastic tensor (C_{11} , C_{22} , C_{33} , C_{44} , C_{55} , C_{66} , C_{12} , C_{13} , C_{23}). The elastic tensor has been estimated by a finite deformation method described in our earlier papers [15, 20]. The calculated elasticity coefficients for a number of hydrostatic pressures are presented in table 4. Comparison of the calculated elasticity coefficient dependence on the pressure for wadsleyite II with the experimental data for anhydrous wadsleyite [21] is presented in figure 5. To our best knowledge, there is no experimental data on the elasticity tensor for wadsleyite II, and thus, we have used an anhydrous wadsleyite phase at pressures up to 15 GPa [21] as reference in the following comparisons. The elasticity coefficients of wadsleyite II are similar to these of wadsleyite, furthermore the values of the computed $C_{ij}(P)$ extrapolated to $P = 0$ GPa are

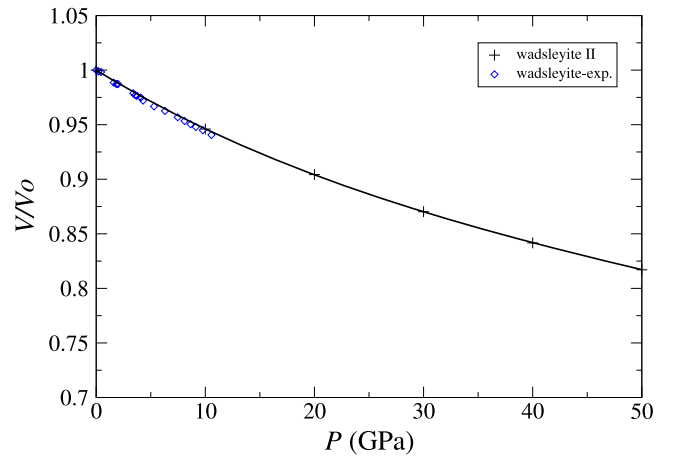


Figure 4. Calculated equation of state for the anhydrous wadsleyite II structure. The third order BM EOS fit to relative unit cell volume compressibility is marked by a solid line while crosses correspond to the computed points. The zero pressure volume from the calculation is $V_0 = 1372 \text{ \AA}^3$. Diamonds represent the experimental volume compressibility for the hydrous phase of wadsleyite II (data from [7]).

in good agreement with experimental data [21]. The relative difference is below 10% (see table 5).

Moreover, the determinant $\det C_{ij}(P) > 0$ and the minor determinants of the $C_{ij}(P)$ elasticity tensor are positive ($C_{11}(P)$, $C_{44}(P)$, $C_{55}(P)$, $C_{66}(P) > 0$), indicating that the wadsleyite II structure is stable with respect to unit cell deformations at pressures in the calculation range (0–25 GPa). The chosen upper pressure 25 GPa is critical in the scope of phase stability and the coexistence of Mg_2SiO_4 polymorphs [4, 7, 22, 23] and thus also appropriate for an upper limit of the elastic constant calculations, since the pressures above this limit are, basically, non-physical for this compound.

Table 3. Comparison of the bulk moduli hydrous and anhydrous phases of wadsleyite and wadsleyite II. The hydrous phase bulk moduli are dependent on wt% of H₂O content. The bulk modulus from static calculation (at $T = 0$ K) is denoted by *, otherwise values are determined at ambient temperature.

	H ₂ O (wt%)	K_T (GPa)	K'_T
Anh. wadsleyite II	—	160 ± 10^a	—
Anh. wadsleyite II*	—	160.1^b	4.3^b
Hyd. wadsleyite II	2.1^a	151 ± 6^a	6 ± 2.5^a
	2.8^a	145.6 ± 2.8^a	6.1 ± 0.7^a
Anh. wadsleyite	—	172^c	4.2^c
Hyd. wadsleyite	2.5 ± 0.3^d	155 ± 2^d	4.3^d
	0.005^e	173^e	4.1^e
	0.38^e	161^e	5.4^e
	1.18^e	158^e	4.2^e
	1.66^e	154^e	4.9^e

^a Smyth *et al* [7]. ^b Calculation in present work. ^c Li *et al* [17].

^d Yusa *et al* [18]. ^e Holl *et al* [25].

Table 4. Elasticity tensor $C_{ij}(P)$ (GPa) of wadsleyite II structure calculated for several pressures.

P (GPa)	C_{11}	C_{22}	C_{33}	C_{44}	C_{55}	C_{66}	C_{12}	C_{13}	C_{23}
4.30	379	373	289	115	123	106	78	104	106
8.69	408	401	324	123	132	119	90	110	118
13.10	437	430	355	131	140	130	101	118	128
20.00	481	470	400	142	151	147	120	132	144
24.53	508	496	428	149	158	157	132	141	156

We have also determined the synthetic elastic parameters derived from elasticity tensor elements $C_{ij}(P)$: the bulk modulus

$$K = \frac{1}{9}(C_{11} + C_{22} + C_{33}) + \frac{2}{9}(C_{12} + C_{23} + C_{31}), \quad (2)$$

the shear modulus

$$\mu = \frac{1}{15}(C_{11} + C_{22} + C_{33}) - \frac{1}{15}(C_{12} + C_{23} + C_{31}) + \frac{3}{15}(C_{44} + C_{55} + C_{66}), \quad (3)$$

Poisson's ratio

$$\sigma = \frac{1}{2} \frac{3K - 2\mu}{3K + 2\mu}, \quad (4)$$

and Young's modulus

$$E = 2\mu(1 + \sigma). \quad (5)$$

These elastic parameters are compared with the experimental data [21] in figure 6,

We can also derive further data from the calculated quantities. The propagation velocities of the compression waves v_p and the shear waves v_s can be calculated from the elastic moduli using standard expressions:

$$v_p = \sqrt{\frac{3K + 4\mu}{3\rho}}; \quad v_s = \sqrt{\frac{\mu}{\rho}}. \quad (6)$$

A comparison of the calculated aggregate velocities for wadsleyite II in the pressure interval 0–25 GPa and the experimental acoustic velocities for the wadsleyite phase measured using Brillouin scattering in a diamond anvil

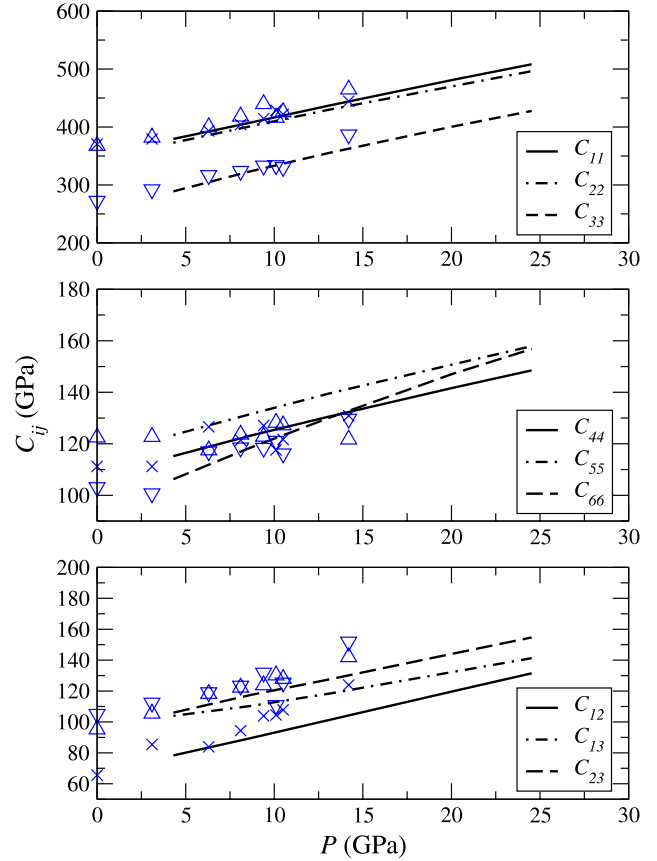


Figure 5. Comparison of calculated elastic constants of wadsleyite II with laboratory measurements of the wadsleyite structure (data from [21]). The solid lines represent the linear regression fit to calculated $C_{ij}(P)$. Crosses (C_{11} , C_{44} , C_{12}), triangles up (C_{22} , C_{55} , C_{13}) and triangles down (C_{33} , C_{66} , C_{23}) show the experimental values for wadsleyite structure.

cell [21] is presented in figure 7. A summary of the calculated parameters for elasticity moduli, material densities and wave velocities is included in table 6. The compressional and shear wave velocities and their pressure derivatives have been estimated from linear regression as $v_p = 9.62 \text{ km s}^{-1}$, $v'_p = 0.06 \text{ km s}^{-1} \text{ GPa}^{-1}$ and $v_s = 5.73 \text{ km s}^{-1}$, $v'_s = 0.03 \text{ km s}^{-1} \text{ GPa}^{-1}$ respectively and are in agreement with the results of previous theoretical study of the Mg_2SiO_4 wadsleyite phase [24].

7. Conclusions

The model structure of anhydrous wadsleyite II with chemical formula Mg_2SiO_4 has been constructed and its structural stability and elasticity properties have been investigated from first principles using the DFT + GGA method. A stable lattice structure at range of pressures of $P = 0\text{--}30$ GPa has been found, and confirmed by the lattice dynamics calculations. Indeed, PDOS contained no imaginary frequencies, which indicates that the crystal structure of anhydrous wadsleyite II is stable in the investigated range of pressures (0–30 GPa). The pressure dependence of the cell volume, lattice parameters and density has been also determined and fitted to the third

Table 5. Comparison of elasticity constants $C_{ij}(P)$ (GPa) of wadsleyite II structure extrapolated to $P = 0$ GPa with experimental values at $P = 0$ GPa for anhydrous wadsleyite [21].

	P (GPa)	C_{11}	C_{22}	C_{33}	C_{44}	C_{55}	C_{66}	C_{12}	C_{13}	C_{23}
Anh. wadsleyite	0	370.5	367.7	272.4	111.2	122.5	103.1	65.6	95.2	105.1
Wadsleyite II—this study	0	352	348	263	109	117	96	67	95	96

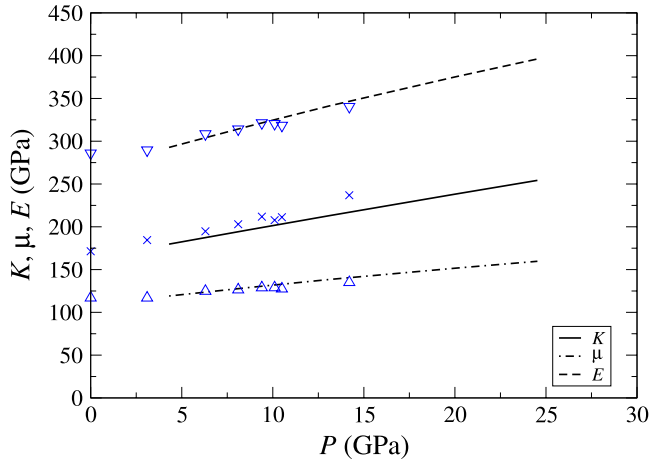


Figure 6. Comparison of calculated elastic parameters of wadsleyite II with experimental measurements of the anhydrous wadsleyite structure (after [21]). The experimental values for wadsleyite are denoted by crosses (bulk modulus K), up triangles (shear modulus μ) and down triangles (Young's modulus E), while values calculated for wadsleyite II are drawn as solid, dash-dotted and dashed lines, respectively.

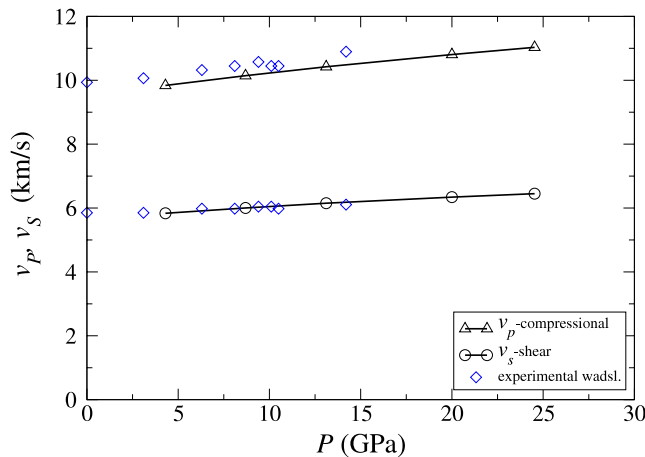


Figure 7. Comparison of computed compressional and shear velocities of the anhydrous wadsleyite II structure, depicted by triangles up and circles, respectively, with the experimentally determined anhydrous wadsleyite (Zha et al) [21] data, represented by diamonds.

order Birch–Murnaghan equation of state. A number of elasticity properties, including elastic moduli and seismic velocities, has been determined by application of the finite deformation method for hydrostatic pressures up to 25 GPa. The comparison of calculated results for wadsleyite II with previous data for the wadsleyite phase shows that the elasticity properties, density and aggregate velocities of the anhydrous

Table 6. Wadsleyite II densities, elastic moduli K , E , μ , Poisson's ratio σ and speed of sound waves v_p , v_s at pressures up to 25 GPa.

P (GPa)	ρ (kg m ⁻³)	K (GPa)	μ (GPa)	σ	E (GPa)	v_p (km s ⁻¹)	v_s (km s ⁻¹)
4.30	3499	179.74	119.15	0.229	292.77	9.84	5.83
8.69	3581	196.45	129.04	0.231	317.58	10.14	6.00
13.10	3659	212.96	138.38	0.233	341.23	10.42	6.15
20.00	3770	238.1	151.56	0.247	375.1	10.80	6.34
24.53	3838	254.22	159.68	0.240	396.1	11.03	6.45

wadsleyite II structure are very close to those of anhydrous wadsleyite. The derived structural and mechanical properties could be used for possible detailed seismological studies of the transition zone structure and nature of its discontinuities. There is a possibility that the wadsleyite II phase contributes to the complexity of the magnesium orthosilicate structural phase relations, as an intermediate phase between wadsleyite and ringwoodite fields, with some impact on rheology models.

Acknowledgments

This research was supported by the Marie Curie Research and Training Network under Contract No. MRTN-CT-2006-035957 project c2c (crust to core) and Polish Ministry of Science and Education Grant No. 541/6.PR UE/2008/7.

References

- [1] Anderson D L 1989 *Theory of the Earth* (Boston, MA: Blackwell) p 366
- [2] Dziewonski A M and Anderson D L 1981 *Phys. Earth Planet. Inter.* **25** 297
- [3] Ringwood A E 1975 *Composition and Petrology of the Earth's Mantle* (New York: McGraw-Hill) chapter 14-3
- [4] Smyth J R and Kawamoto T 1997 *Earth Planet. Sci. Lett.* **146** E9
- [5] Horioka K, Takahashi K, Morimoto N, Horiuchi H, Akaogi M and Akimoto S 1981 *Acta Crystallogr. B* **37** 635
- [6] Akaogi M, Akimoto S, Horioka H, Takahashi K and Horiuchi H 1982 *J. Solid State Chem.* **44** 257
- [7] Smyth J R, Holl C M, Langenhorst F, Laustsen H M S, Rossman G R, Kleppe A, McCammon C A, Kawamoto T and van Aken P A 2005 *Phys. Chem. Miner.* **31** 691
- [8] Baosheng L 2003 *Am. Mineral.* **88** 1312
- [9] Dziewonski A M, Hales A L and Lapwood E R 1975 *Phys. Earth Planet. Inter.* **10** 12
- [10] Perdew J P, Burke K and Ernzerhof M 1996 *Phys. Rev. Lett.* **77** 3865
- [11] Kresse G and Hafner J 1993 *Phys. Rev. B* **47** 558
Kresse G and Hafner J 1994 *Phys. Rev. B* **49** 14251

- Kresse G and Furthmüller J 1999 *Software VASP* IMP-UW, Vienna
- Kresse G and Furthmüller J 1996 *Phys. Rev. B* **54** 11169
- Kresse G and Furthmüller J 1996 *Comput. Mater. Sci.* **6** 15
- [12] Monkhorst H J and Pack J D 1976 *Phys. Rev. B* **13** 5188
- [13] Parlinski K, Li Z Q and Kawazoe Y 1997 *Phys. Rev. Lett.* **78** 4063
- [14] Parlinski K 2008 *PHONON Software* Cracow, Poland
- [15] Jochym P T, Parlinski K and Krzywiec P 2004 *Comput. Mater. Sci.* **29** 414
- [16] Jochym P T and Parlinski K 2000 *Eur. Phys. J. B* **15** 265
- [17] Li B, Liebermann R C and Weidner D J 1998 *Science* **281** 675
- [18] Yusa H and Inoue T 1997 *Geophys. Res. Lett.* **24** 1831
- [19] Mao Z, Jacobsen S D, Jiang F, Smyth J R, Holl C M and Duffy T S 2008 *Geophys. Res. Lett.* **35** L21305
- [20] Jochym P T, Parlinski K and Sternik M 1999 *Eur. Phys. J. B* **10** 9
- [21] Zha Ch, Duffy T S, Mao H, Downs R T, Hemley R J and Weidner D J 1997 *Earth Planet. Sci. Lett.* **147** E9
- [22] Akaogi M, Ito E and Navrotsky A 1989 *J. Geophys. Res.* **94** 15671
- [23] Katsura T and Ito E 1989 *J. Geophys. Res.* **94** 15663
- [24] Kiefer B, Stixrude L, Hafner J and Kresse G 2001 *Am. Mineral.* **86** 1387
- [25] Holl C M, Smyth J R, Jacobsen S D and Frost D J 2008 *Am. Mineral.* **93** 598